Electronic Supplementary Material (ESI) for Dalton Transactions

Supplementary information for

"Influence of Ferromagnetic Connection of Ising-type Dy^{III}-based Single Ion Magnets on their magnetic slow relaxation"

X. Yi, K. Bernot, O. Cador J. Luzon, G. Calvez, C. Daiguebonne and O.Guillou*

1. Experimental procedures
2. Additional figures and tables

1. Experimental procedures

Synthesis. Hexafluoroacetylacetone is reacted with $DyCl_3 \cdot 6H_2O$ to form $Dy(hfac)_3 \cdot 2H_2O$. [1] 0.1 mmol of this precursor is then dissolved in boiling hexane (20 mL). After stirring for 2 hours, 4-styrylpyridine (0.1 mmol) in hexane (20 mL) is added and refluxed for 30 minutes. Then the solution is cooled to 4°C for slow evaporation and gives colourless crystals (**1**) suitable for single crystal X-ray analysis. Elemental analysis calcd (%) for **1**; C: 34.22, H: 1.64, N: 1.42; found: C 34.12, H 1.57, N 1.39.

Crystal Structure Determination. Single crystal was mounted on a APEXII AXS-Bruker diffractometer equipped with a CCD camera and a graphite-monochromated MoKα radiation source (λ=0.71073 Å), from the Centre de Diffractométrie (CDIFX), Université de Rennes 1, France. Data were collected at 150K. Structure was solved with a direct method using the SIR-97 program[2] and refined with a full-matrix least-squares method on F^2 using the SHELXL-97 program[3] and WinGx interface.[4] Crystallographic data are summarized in Table 1. CCDC-893273 contains the supplementary crystallographic data for this paper. These data can be obtained free of charge from The Cambridge Crystallographic Data Centre via www.ccdc.cam.ac.uk/data_request/cif.

X-ray Powder Diffraction. Diagrams have been collected using a Panalytical X'Pert Pro diffractometer with an X'Celerator detector. The typical recording conditions were 45kV, 40mA for Cu-Kα (λ=1.542Å), the diagrams were recorded in θ-θ mode in 60 min between 5° and 75° (8378 measurements) with a step size of 0.0084° and a scan time of 50s. The calculated patterns were produced using the Powdercell and WinPLOTR software programs.[5]

Scanning Electron Microscopy (SEM) and Energy Dispersive Spectroscopy (EDS) analysis All measurements were carried out with a Hitachi TM-1000, Tabletop Microscope version 02.11 (Hitachi High-Technologies, Corporation Tokyo Japan) with EDS analysis system (SwiftED-TM, Oxford Instruments Link INCA). The detector type is a Silicon drift detector, with an energy resolution of 165eV which allows us to detect the element from Na to U. With the software SwiftED-TM, qualitative and quantitative analyses can be realized. All the samples have been observed by means of an electron beam accelerated at 15kV, under high vacuum. The samples were assembled on carbon discs, stuck on an aluminium stub fixed at 7mm from EDX beam, with an angle of measurement of 22°.

Magnetic dc and ac Measurements. Bulk measurements were performed on polycrystalline sample embedded in grease to avoid in-field orientation of the crystallites. A Quantum Design MPMS magnetometer has been used. Measurements were corrected for the diamagnetic contribution, as calculated with Pascal's constants, and for the diamagnetism of the sample holder, as independently determined. Single crystal measurements were performed on the same magnetometer equipped with a horizontal rotating sample holder. After indexation of the crystal faces by single crystal diffraction, the angular dependence of the magnetization has been measured in three orthogonal planes (ab', b'c' and ac') at 2 K with a 1 kOe magnetic field. c' vector is collinear to (011) direction. The data were then fitted assuming that M = χH. Rotation of H in $\alpha\beta$ plane turns the expression of the magnetization to $M/H = \chi_{\alpha\,\alpha}(\cos\theta)^2 + \chi_{\beta\beta}(\sin\theta)^2 + \chi_{\alpha\,\beta}(\sin\theta\cos\theta)$ where α and β are the directions of the vectors a, b' and c' in a cyclic permutation and θ is the angle between H and α direction.

2. Additional figures and tables

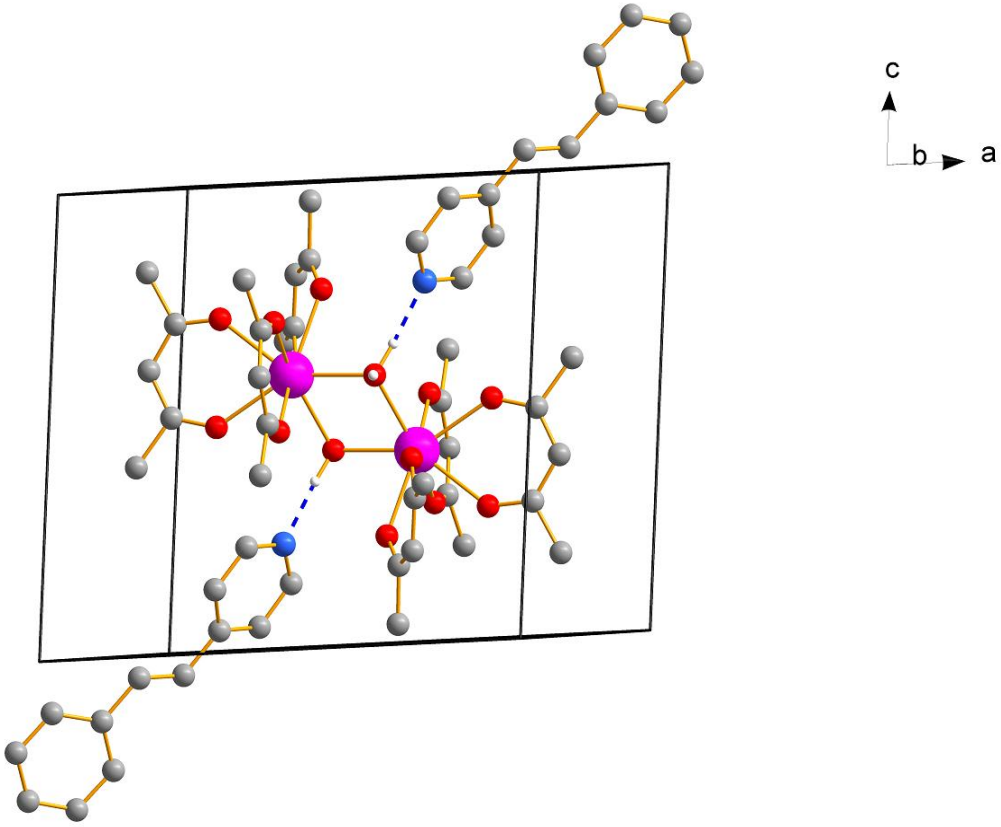

Figure S1: View of **1** highlighting the weak N-H bonds. Hydrogen and fluorine atoms are omitted for clarity.

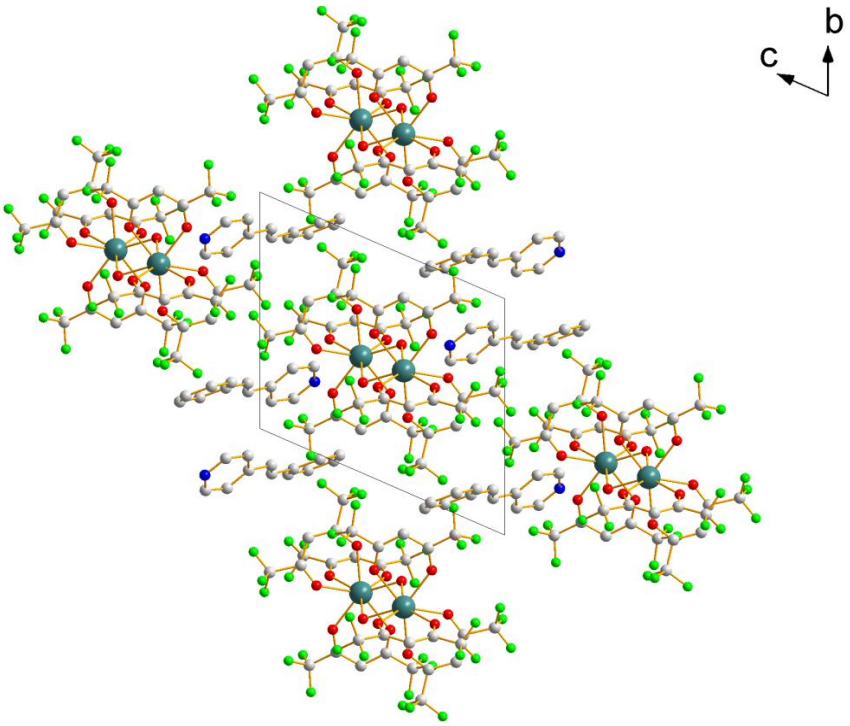

Figure S2: View of the crystal packing of $[Dy(hfac)_3H_2O]_2$ along a axis. Hydrogen atoms are omitted for clarity.

Table S1: Main crystallographic parameters for **1**

Formula	$C_{28}\ H_{16}\ F_{18}\ O_7\ N\ Dy$
M ($g.mol^{-1}$)	982.92 $g.mol^{-1}$
Crystal system	triclinic
Space group	P-1 (N°2)
a(Å)	12.69(4)
b(Å)	12.79(0)
c(Å)	13.04(7)
α(°)	64.79
β(°)	81.14
γ(°)	64.31
V(Å)	1725.9(0)
Z	2
T(K)	150(2)
2θ range (°)	4.06-54.90
Reflns collected	21264
Independent	7840
Observed reflns	6453
Parameters	496
$R_{int}/R_1/\omega R^2$	0.0351/0.0340/0.093
Goof	1.092

Table S2: Selected planes angles, bond and distances.

Planes (numbered by their oxygen atoms)	Angle (°)	Bond	Distance (Å)	Atoms	Angle (°)
727b-217b	13.32 (4)	Dy1-Dy1	3.78(1)	O2-Dy1-O1	71.55(3)
354-546	6.22 (9)	Dy1-O3	2.38 (2)	O7-Dy1-O7b	72.12(8)
752-523	54.22 (1)	Dy1-O6	2.40(8)	O2-Dy1-O7	77.27(8)
523-231	53.95 (1)	Dy1-O7	2.33(9)	O7b-Dy1-O1	73.32(9)
213-134	49.92 (5)	Dy1-O4	2.39(8)	O3-Dy1-O4	70.21(3)
314-147b	47.57 (9)	Dy1-O2	2.36(9)	O4-Dy1-O6	73.06(4)
147b-647b	52.49 (8)	Dy1-O1	2.37(5)	O6-Dy1-O5	70.94(1)
476-767	52.21 (5)	Dy1-O5	2.36(1)	O5-Dy1-O3	72.01(1)
767b-765	53.30 (5)			O7b-Dy1-O6	80.60 (6)
657-572	46.84 (6)			O7-Dy1-O6	79.78(6)
				O3-Dy1-O1	77.25(1)
				O4-Dy1-O1	84.68(2)

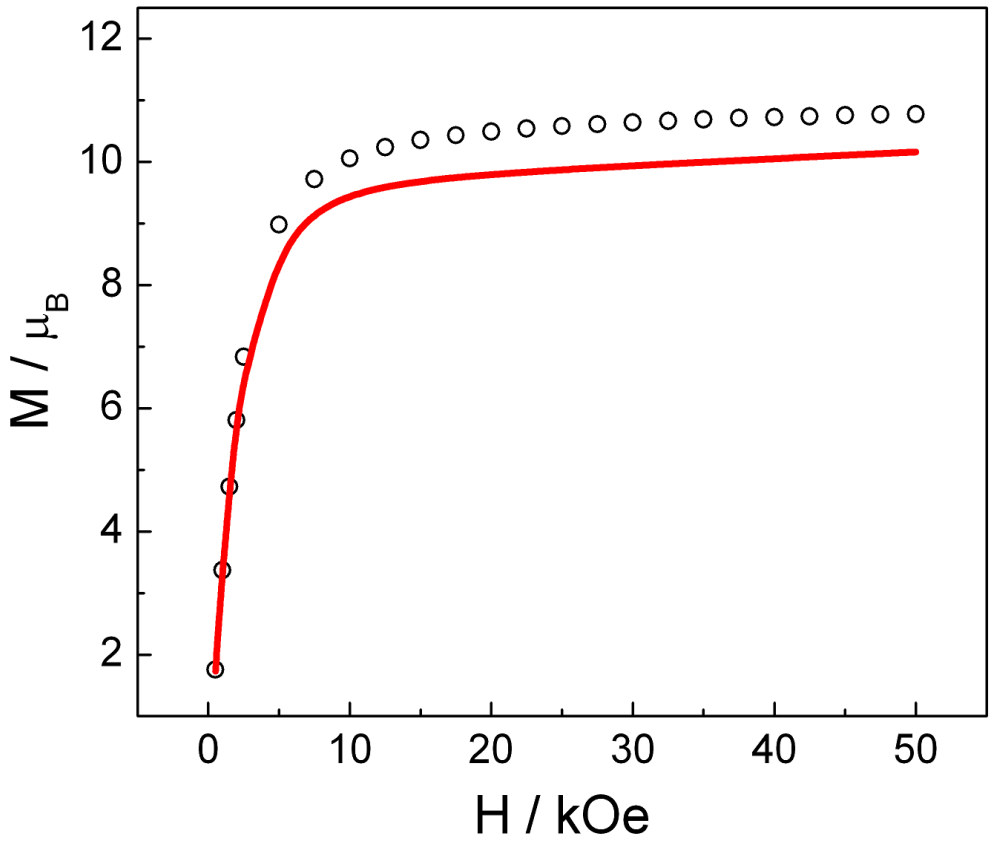

Figure S3: Field dependence of the magnetization measured on **1** with best fit.

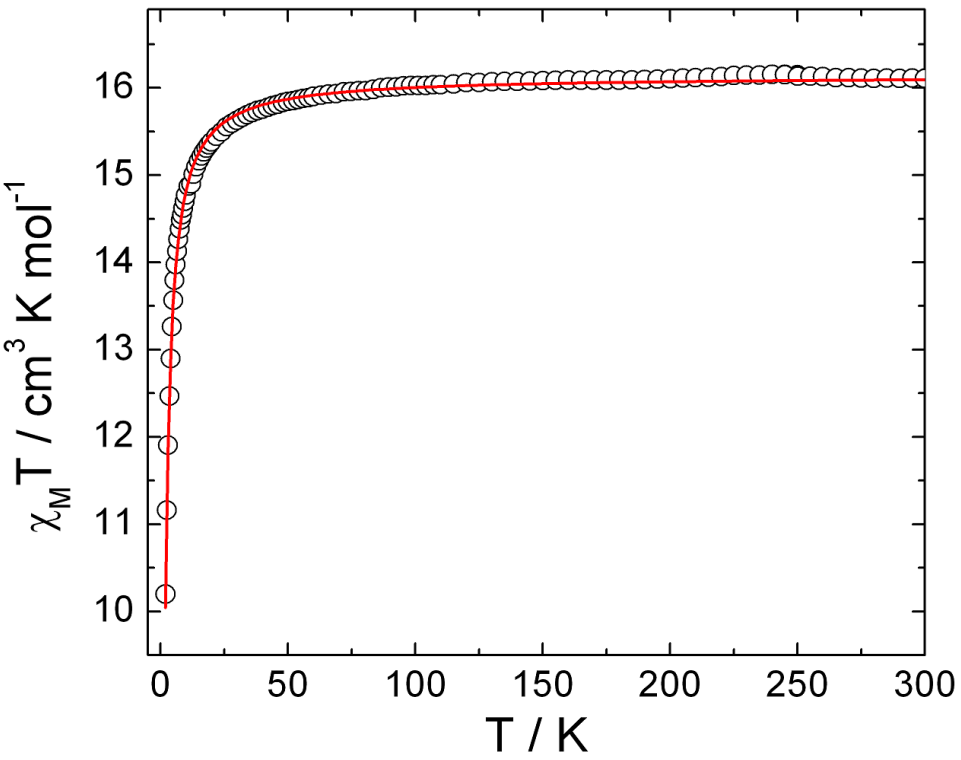

Figure S5: Temperature dependence of $\chi_M T$ for **3** with best fit as solid line.

Estimation of the dipolar contribution to the magnetic coupling constant.

The dipolar magnetic interaction between two magnetic moments can be written as:

$$H = -\frac{\mu_0}{4\pi r^3}\left(3(\vec{m}_1 \cdot \hat{r})(\vec{m}_2 \cdot \hat{r}) - \vec{m}_1 \cdot \vec{m}_2\right)$$

For a trivalent lanthanide ion: $\vec{m} = g_J \beta \vec{J}$. So,

$$H = -\frac{\mu_0 (g_J \beta)^2}{4\pi r^3}\left(3(\vec{J}_1 \cdot \hat{r})(\vec{J}_2 \cdot \hat{r}) - \vec{J}_1 \cdot \vec{J}_2\right)$$

In the Dy dimer, **1**, considering only the ground doublet state in which both easy anisotropy axes are parallel, the interaction can be written as:

$$H = -\frac{\mu_0 (g_J \beta)^2}{4\pi r^3}\left(3\cos^2\theta - 1\right) J_{z1} \cdot J_{z2} = -A\left(3\cos^2\theta - 1\right) J_{z1} \cdot J_{z2}$$

$\frac{\mu_0}{4\pi}$ is an adimensional constant: 10^{-7}

β is the Bohr magneton: 9.27400915(23)×10^{-24} J/T.

For the ground state multiplet of the Dy(III) ion: g_J=4/3.

Replacing the different values the value of A in the previous expression is 0,01424 cm^{-1} (for r=3,78 A). Then, the contribution of the dipolar interaction to the magnetic coupling constant should be:

$J_{dip} = A\left(3\cos^2\theta - 1\right)$

For θ =51.2°, J_{dip}=0.0025 cm^{-1}, value much lower than the value obtained from the fit: J=0.01005 cm^{-1}.

For the Gd derivative, **3**, since in Gd(III) $\vec{J} = \vec{S}$, the maximum antiferromagnetic contribution to the antiferromagnetic coupling constant is: J_{dip}=-0,01424 cm^{-1} (when the magnetic moments are collinear and θ =90°).

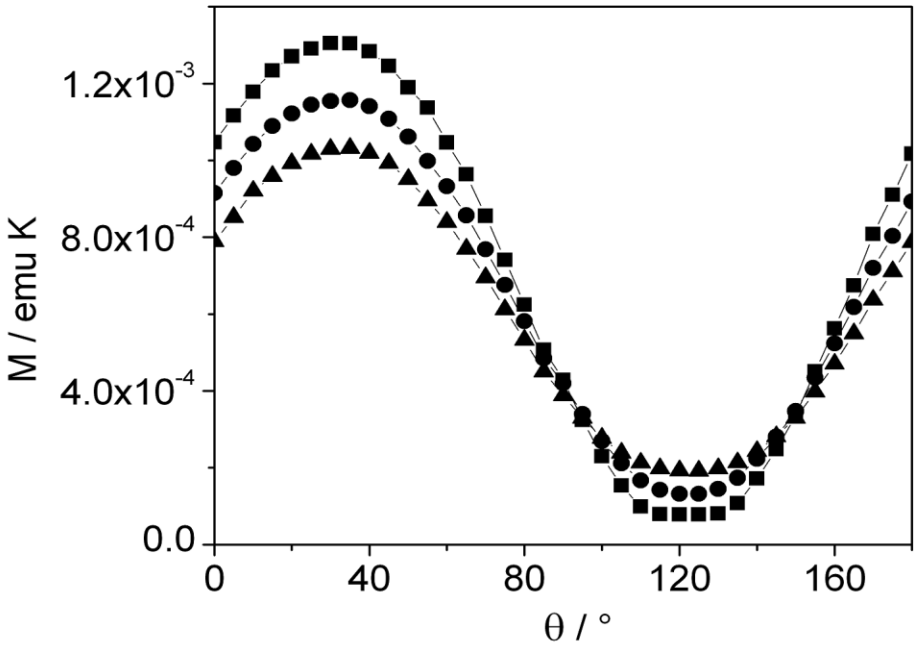

Figure S6: Angular dependence of M measured in the ac' plane of single crystal of **1** recorded at 2 (squares), 5 (circles) and 10 K (triangles).

Susceptibility tensor in the ab'c' frame for compound **1**.

$$\chi_M = \begin{pmatrix} 34.4273 & 3.2491 & -14.3006 \\ 3.2491 & 2.1915 & 1.6354 \\ -14.3006 & 1.6354 & 8.4561 \end{pmatrix} emu\ mol^{-1}$$

Principal values and direction of the susceptibility tensor in the ab'c' frame:

$$\chi_{xx} \begin{pmatrix} 0.224 \\ 0.702 \\ 0.676 \end{pmatrix} = 5.42,\ \chi_{yy} \begin{pmatrix} 0.297 \\ 0.710 \\ -0.638 \end{pmatrix} = -0.02,\ \chi_{zz} \begin{pmatrix} -0.928 \\ -0.058 \\ 0.368 \end{pmatrix} = 44.29\ emu\ mol^{-1}$$

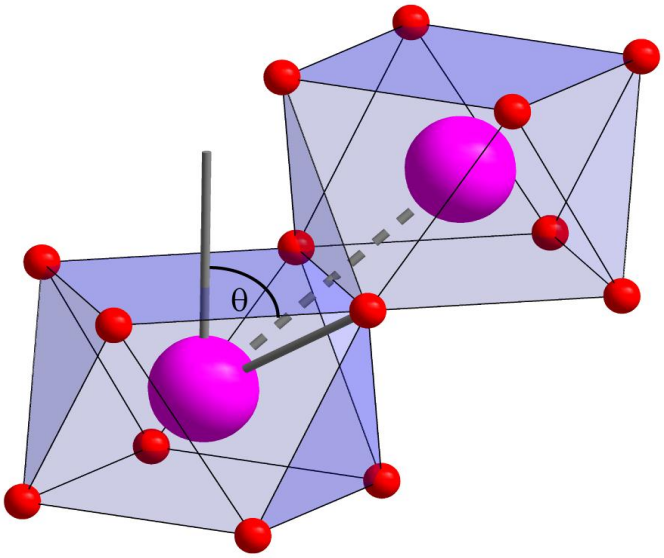

Figure S7: Schematic representation of a centrosymmetrical dimer of ideal SAP sharing an edge of the square face. It is relatively easy to demonstrate that in the hard sphere model the angle (θ) between C_4 axis and metal-metal direction is expressed by $\sin\theta = 2\Big/\sqrt{7-\left(\sqrt{2}-1\right)^2}$ and θ=49.94°.

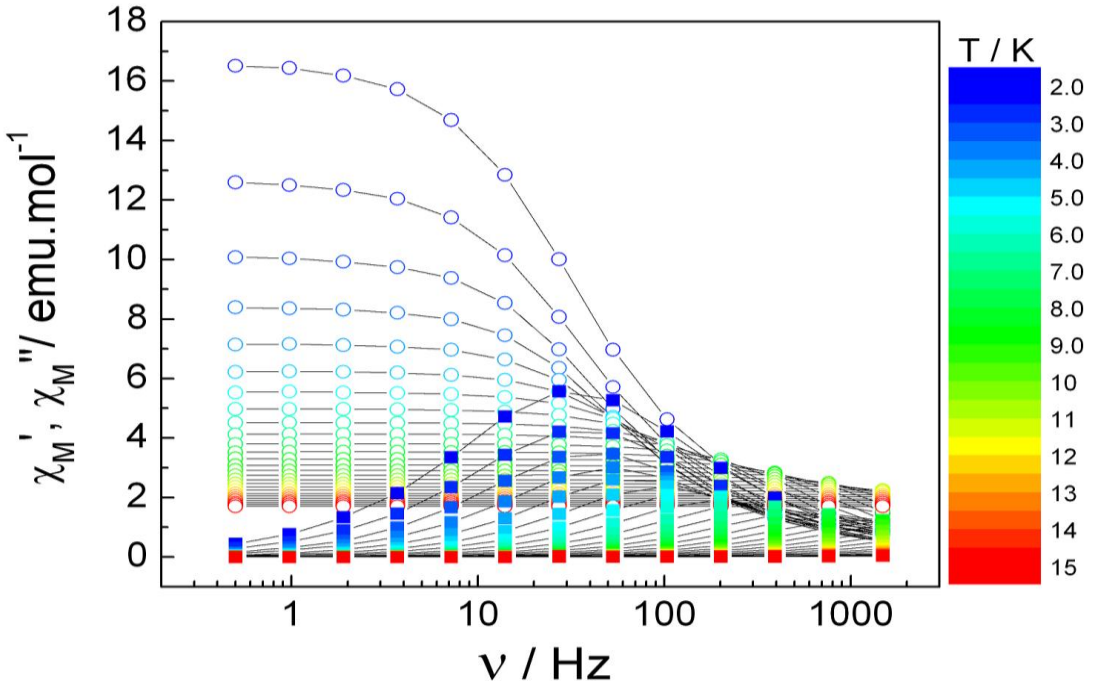

Figure S8: Frequency dependence of χ_M' and χ_M" for **1** measured with 0 Oe external dc field. Colour mapping ranges from 2 (blue) to 15 K (red). Lines are guides to the eye.

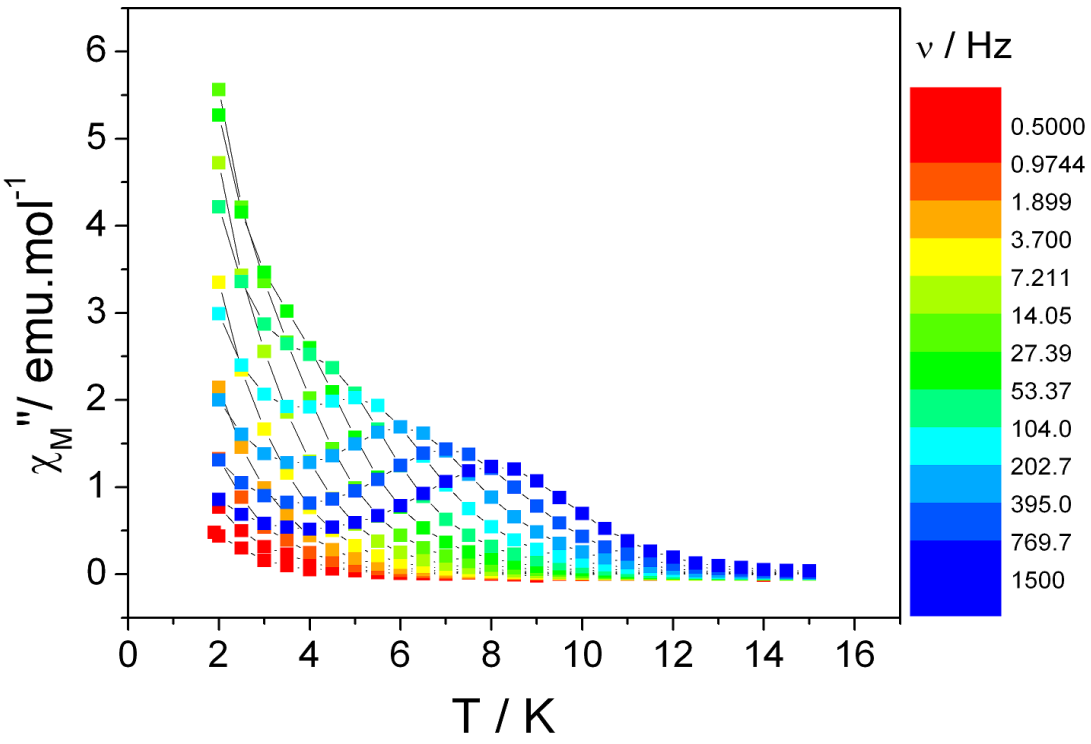

Figure S9: Temperature dependence of χ_M" for **1** measured with 0 Oe external dc field. Colour mapping ranges from 0.5 (red) to 1500 Hz (blue). Lines are guides to the eye.

Table S3: Table of τ extracted values from the fitting of *X'' vs frequency* curves for **1** in 0 Oe dc field.

T(K)	τ (μs)	T(K)	τ (μs)	T(K)	τ (μs)
2	4583	5	1136	8	142
2.5	4086	5.5	803	8.5	97
3	3522	6	564	9	67
3.5	2866	6.5	397	9.5	48
4	2182	7	282	10	27
4.5	1593	7.5	143	10.5	19

Table S4: table of extracted values from the Argand plot of **1** with a 0 Oe external field before normalization.

T (K)	χ_S	χ_T	α	χ^2 (x 10^{-5})
2	1.200 (±0.011)	16.74 (±0.003)	0.207 (±0.008)	1372
2.5	1.010 (±0.008)	12.71(±0.001)	0.196 (±0.007)	691
3	0.891(±0.012)	10.14 (±0.007)	0.173 (±0.004)	816
3.5	0.793 (±0.008)	8.430 (±0.002)	0.150 (±0.002)	465
4	0.722 (±0.009)	7.180 (±0.007)	0.124 (±0.003)	483
4.5	0.661 (±0.007)	6.250 (±0.002)	0.107 (±0.007)	151
5	0.602 (±0.006)	5.553 (±0.001)	0.103 (±0.002)	242
5.5	0.508 (±0.001)	4.977 (±0.003)	0.084 (±0.001)	14
6	0.530 (±0.005)	4.518 (±0.008)	0.086 (±0.004)	32
6.5	0.494 (±0.004)	4.131 (±0.008)	0.081 (±0.001)	82
7	0.440 (±0.002)	3.809 (±0.009)	0.087 (±0.001)	79
7.5	0.376 (±0.001)	3.533 (±0.001)	0.093 (±0.008)	78
8	0.357 (±0.002)	3.295 (±0.002)	0.091 (±0.006)	10
8.5	0.239 (±0.003)	3.087 (±0.006)	0.101 (±0.003)	19
9	0.080 (±0.002)	2.910 (±0.007)	0.130 (±0.002)	68
9.5	0.083 (±0.007)	2.751 (±0.002)	0.180 (±0.004)	188
10	0.032 (±0.009)	2.600 (±0.002)	0.142 (±0.006)	16

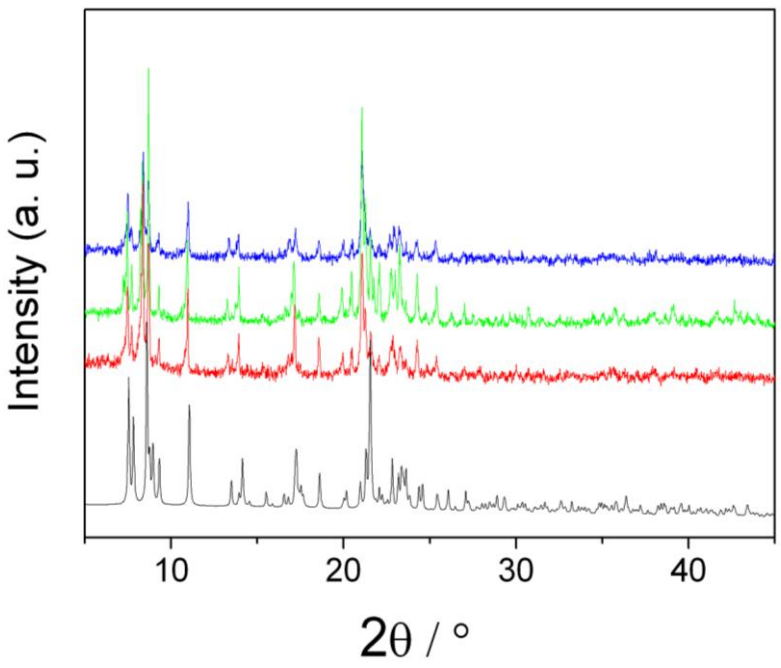

Figure S4: X-Ray powder pattern of **1** simulated from cif file at 150 K (bottom) and **1**, **2** and **3** as powders (from bottom to top) recorded at room temperature.

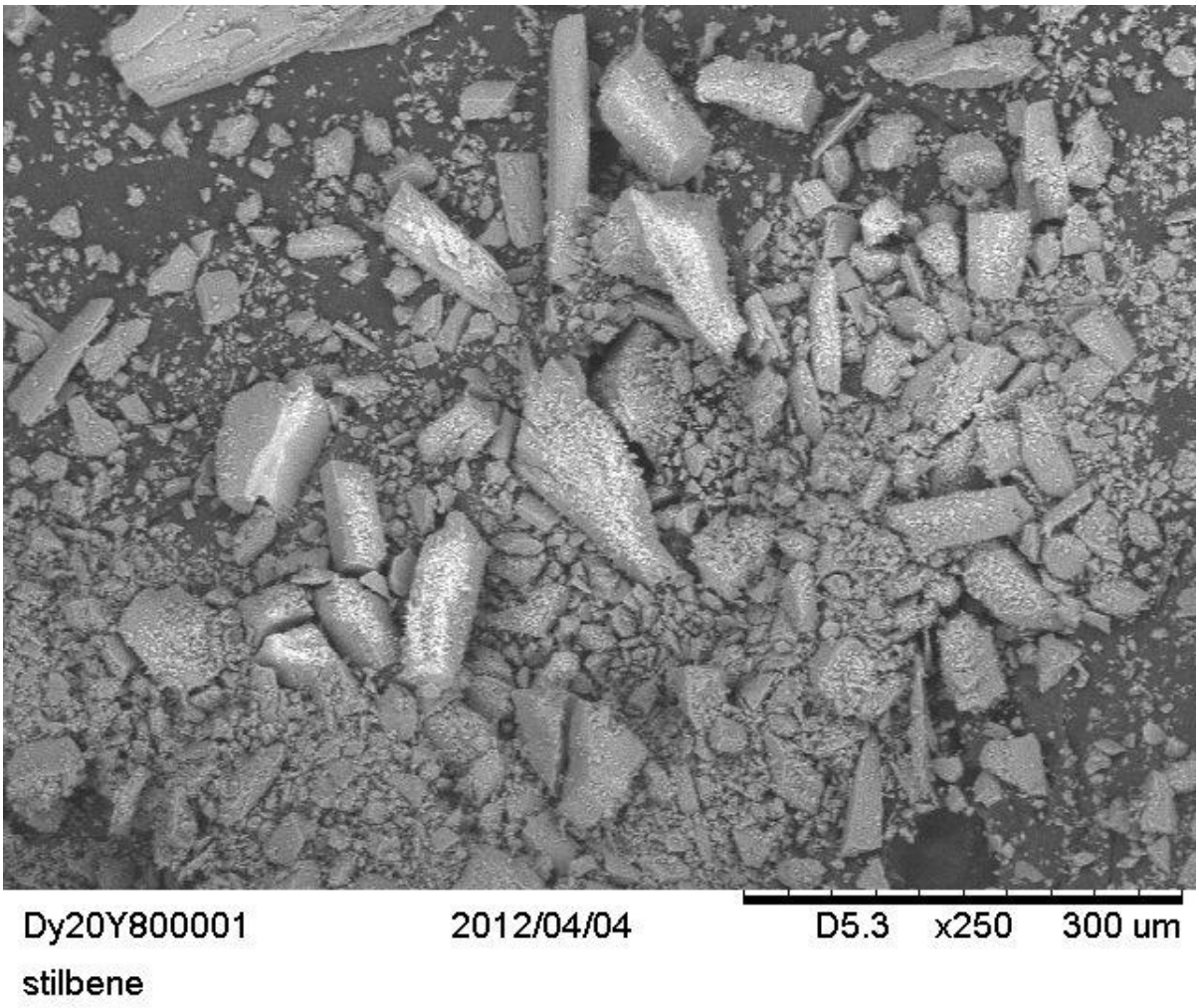

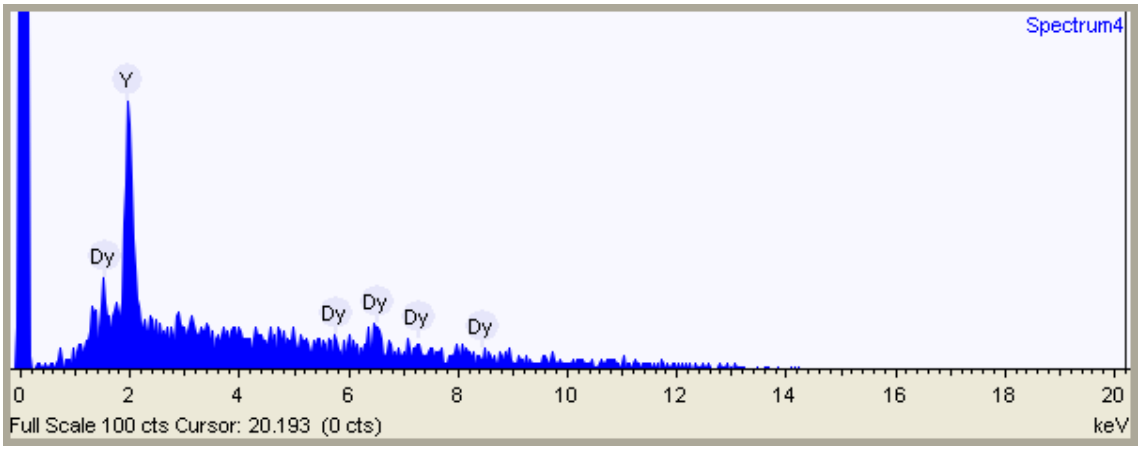

Element	Weight %	atomic
Yttrium	65.7	77.8
Dysprosium	34.3	22.2

Figure S10: SEM images and EDS analysis of the doped sample **2**.

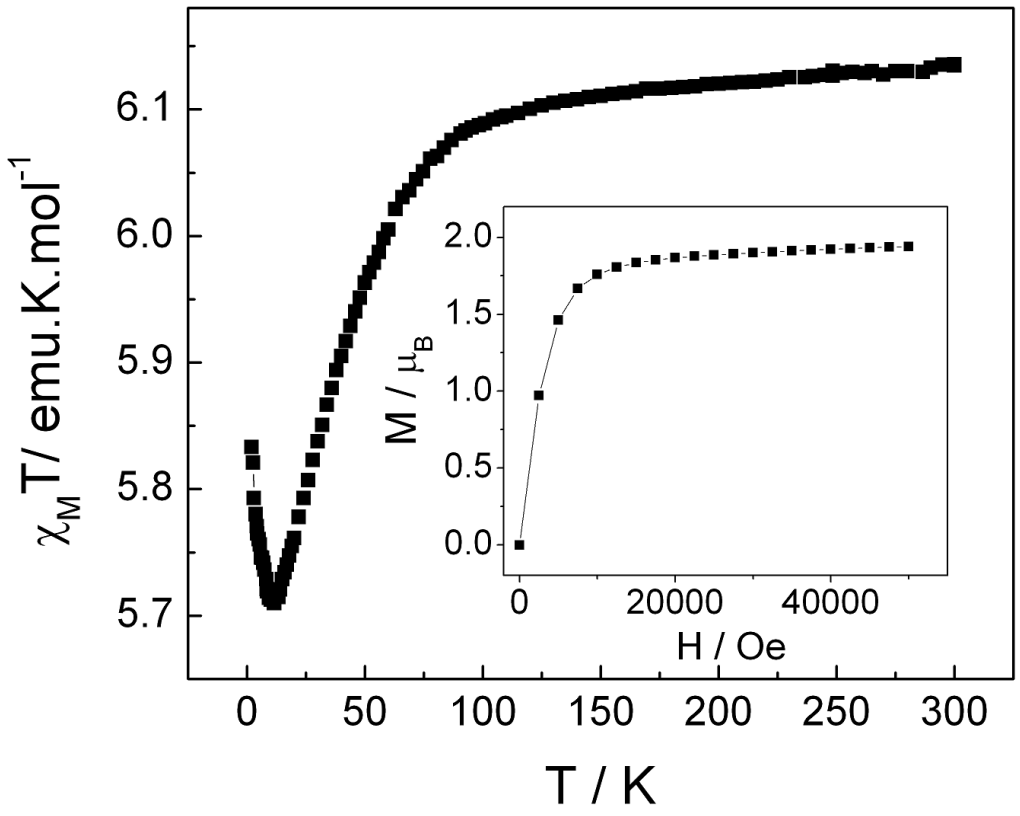

Figure S11: Temperature dependence of $\chi_M T$ for **2**. In inset, field dependence of the magnetization.

The room temperature $\chi_M T_{(RT)}$ value for **2** is 6.13 emu K mol^{-1} in agreement with the measured doping ratio ($Y_{77.5}Dy_{22.5}$) that gives a theoretical $\chi_M T_{(RT)}$ of 6.36 emu.K.mol^{-1}. As for **1** $\chi_M T$ decreases on lowering the temperature, reaches a minimum at 12 K (5.71 emu K mol^{-1}) and then increase at lowest temperature. This last increase is very weak (5.83 emu K mol^{-1} at 2K) and evidences that very few Dy-Dy pairs are present in the sample and that main magnetic entities in **2** are then Dy^{III}-Y^{III} dimers.

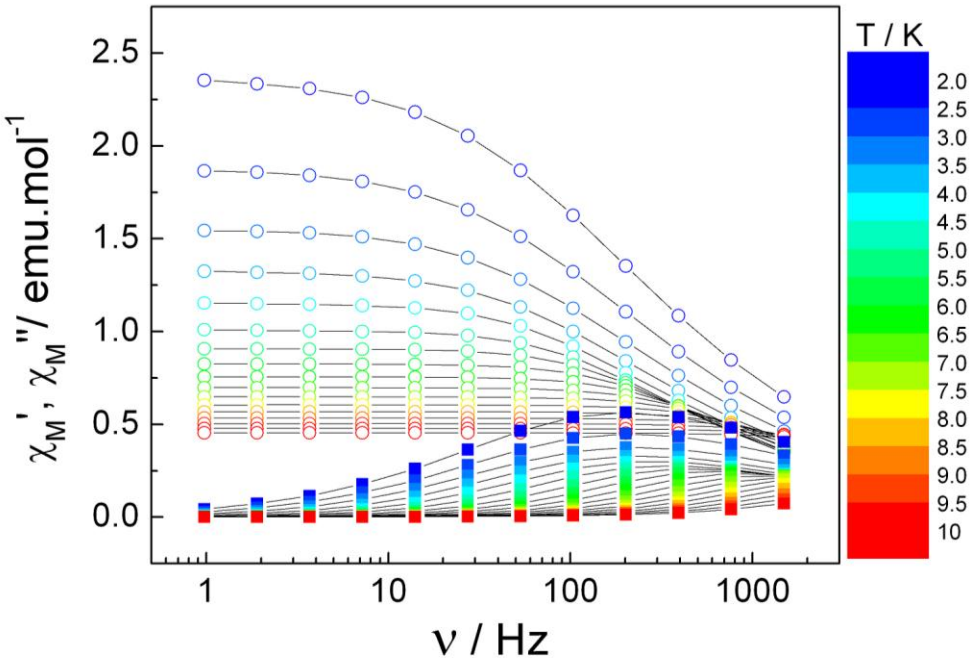

Figure S12: Frequency dependence of χ_M' and χ_M" for **2** measured with 0 Oe external dc field. Colour mapping ranges from 2 (blue) to 15 K (red). Lines are guides to the eye.

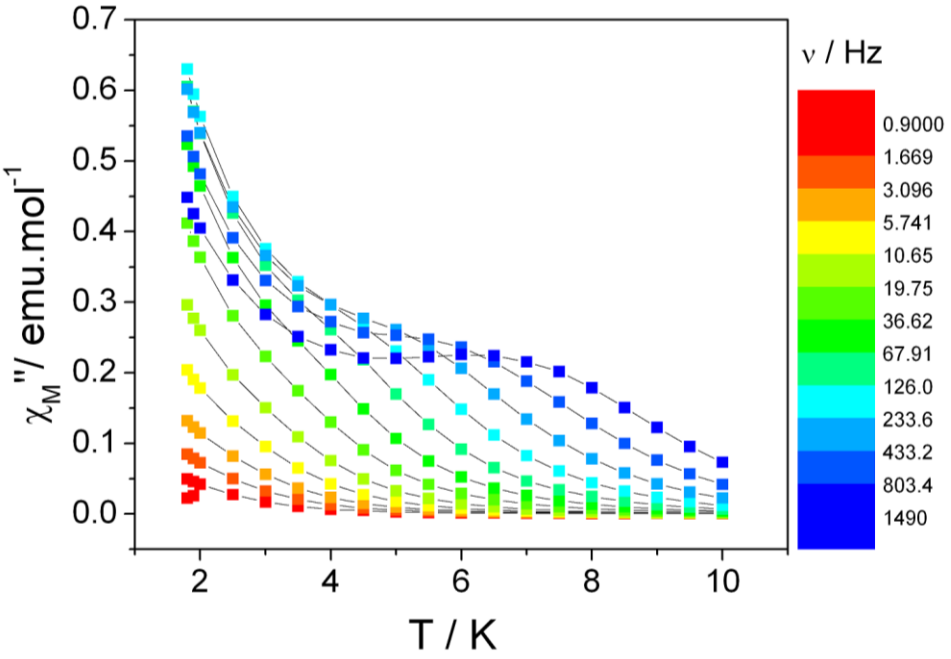

Figure S13: Temperature dependence of χ_M" for **2** measured with 0 Oe external dc field. Colour mapping ranges from 0.9 (red) to 1500 Hz (blue). Lines are guides to the eye.

Table S5: Table of τ extracted values from the fitting of *X'' vs frequency* curves for **2** in 0 Oe dc field.

T(K)	τ (μs)	T(K)	τ (μs)	T(K)	τ (μs)
2	738.2	5	307	8	69
2.5	683	5.5	235	8.5	55
3	615	6	176	9	43
3.5	572	6.5	135	9.5	26
4	484	7	111	10	19
4.5	399	7.5	85		

Table S6: table of extracted values from the Argand plot of **2** with a 0 Oe external field before normalization.

T (K)	χ_s	χ_T	α	χ^2 (x 10^{-5})
2	0.247 (±0.020)	2.393 (±0.007)	0.370 (±0.004)	190
2.5	0.223 (±0.015)	1.897 (±0.005)	0.354 (±0.001)	220
3	0.212(±0.012)	1.566 (±0.005)	0.330 (±0.009)	240
3.5	0.207 (±0.003)	1.335 (±0.001)	0.299 (±0.009)	170
4	0.210 (±0.002)	1.160 (±0.007)	0.250 (±0.008)	180
4.5	0.219 (±0.005)	1.011 (±0.004)	0.177 (±0.007)	140
5	0.207 (±0.001)	0.910 (±0.004)	0.150 (±0.001)	120
5.5	0.196 (±0.008)	0.826 (±0.003)	0.122 (±0.001)	60
6	0.188 (±0.002)	0.756 (±0.009)	0.098 (±0.002)	40
6.5	0.179 (±0.001)	0.698 (±0.005)	0.083 (±0.001)	20
7	0.174 (±0.002)	0.648 (±0.001)	0.068 (±0.004)	10
7.5	0.139 (±0.0007)	0.605 (±0.002)	0.079 (±0.005)	40
8	0.137 (±0.0001)	0.567 (±0.002)	0.061 (±0.004)	0.7
8.5	0.132 (±0.0007)	0.533 (±0.001)	0.055 (±0.002)	0.6
9	0.122 (±0.0001)	0.503 (±0.009)	0.050 (±0.003)	0.3
9.5	0.119 (±0.008)	0.477 (±0.003)	0.043 (±0.002)	0.1
10	0.105 (±0.090)	0.453 (±0.002)	0.041 (±0.001)	0.5

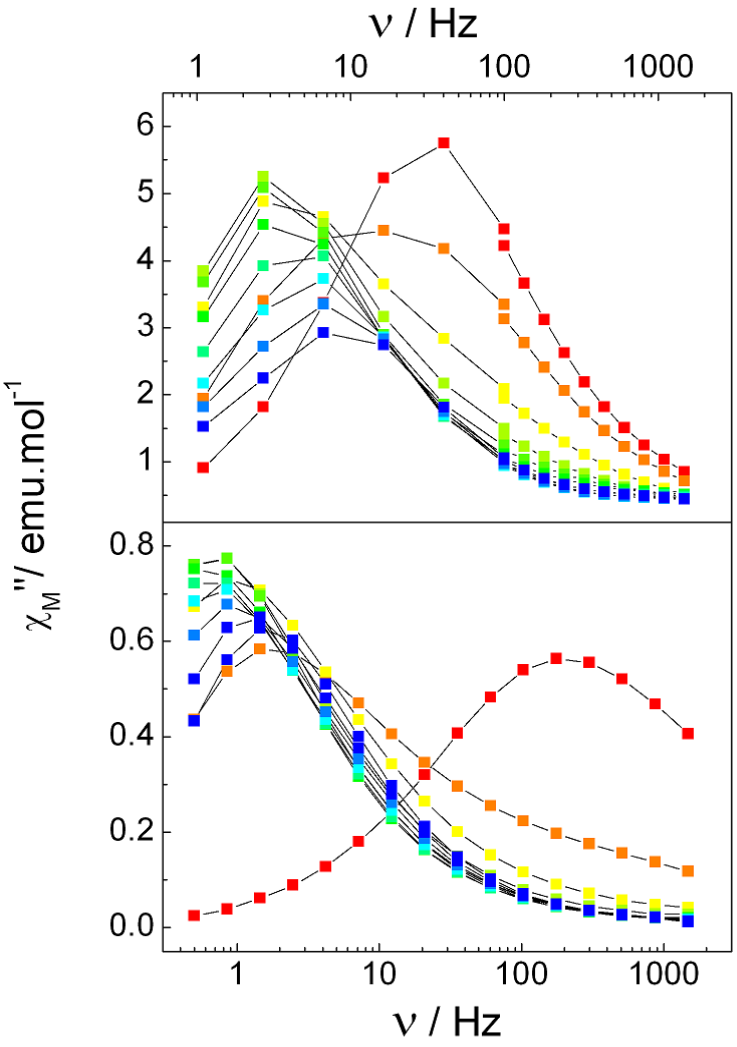

Figure S14: Field dependence of χ_M'' for **1** (top) and **2**(bottom) at 2K. Colour mapping from 0 (red) to 2000 Oe (blue). Lines are guides to the eye.

Table S7: Table of τ extracted values at 2K from the fitting of *X'' vs frequency* curves for **1**. Dc external field varying from 0 to 2800 Oe

H (Oe)	τ (μs) for **1**	τ (μs) for **2**
0	705	11831
200	79927	33603
400	161565	95238
600	218450	115073
800	249020	113000
1000	268641	92093
1200	253214	70845
1400	215484	55766
1600	165164	42760
1800	120758	46065
2000	96988	52574
2200	77588	62892
2400	62318	74944
2600	46406	81946
2800	36164	86986

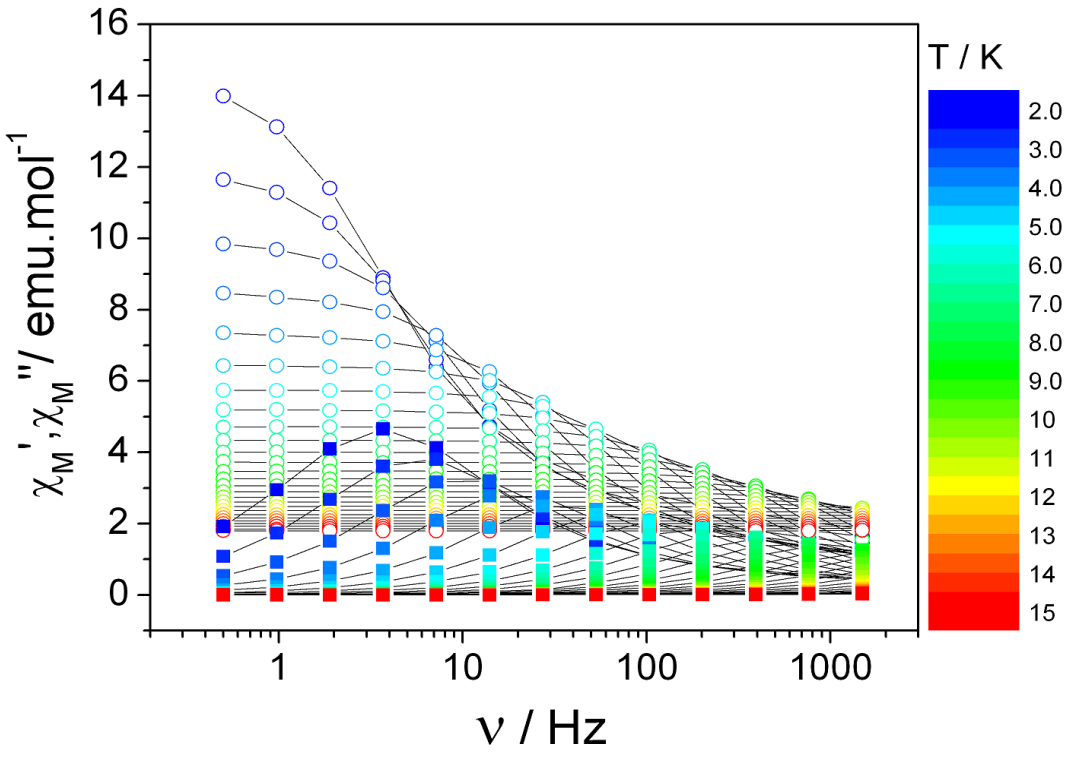

Figure S15: Frequency dependence of χ_M' and χ_M'' for **1** measured with 1000 Oe external dc field. Colour mapping ranges from 2 (blue) to 15 K (red). Lines are guides to the eye.

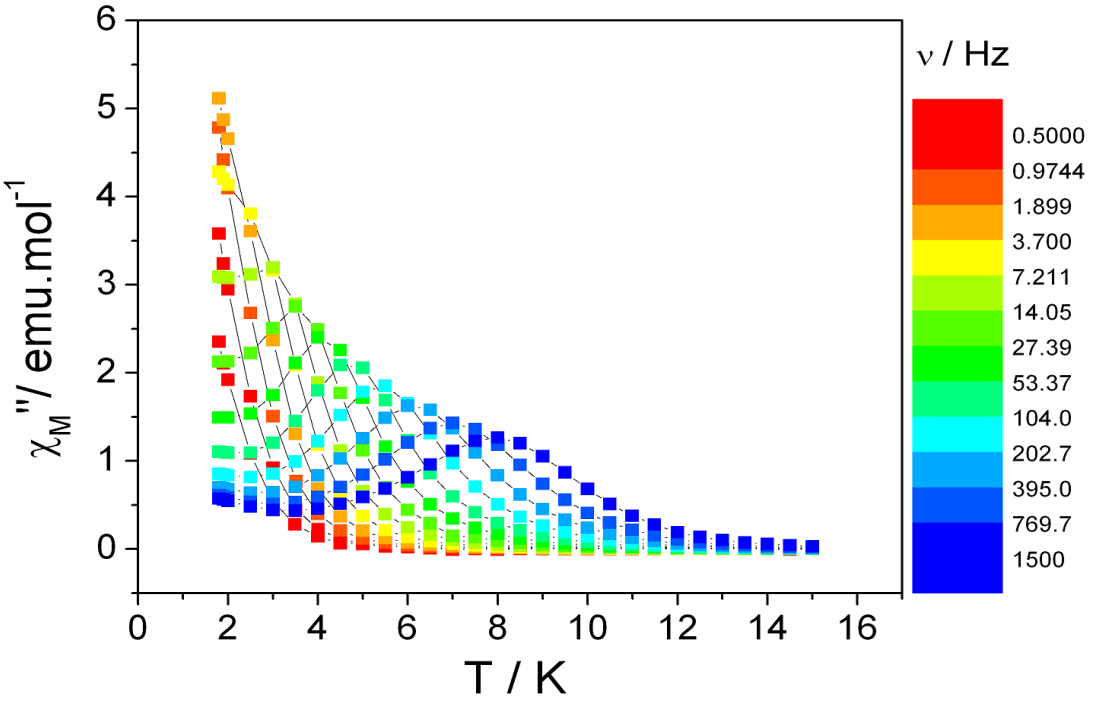

Figure S16: Temperature dependence of χ_M'' for **1** measured with 1000 Oe external dc field. Colour mapping ranges from 0.5 (red) to 1500 Hz (blue). Lines are guides to the eye.

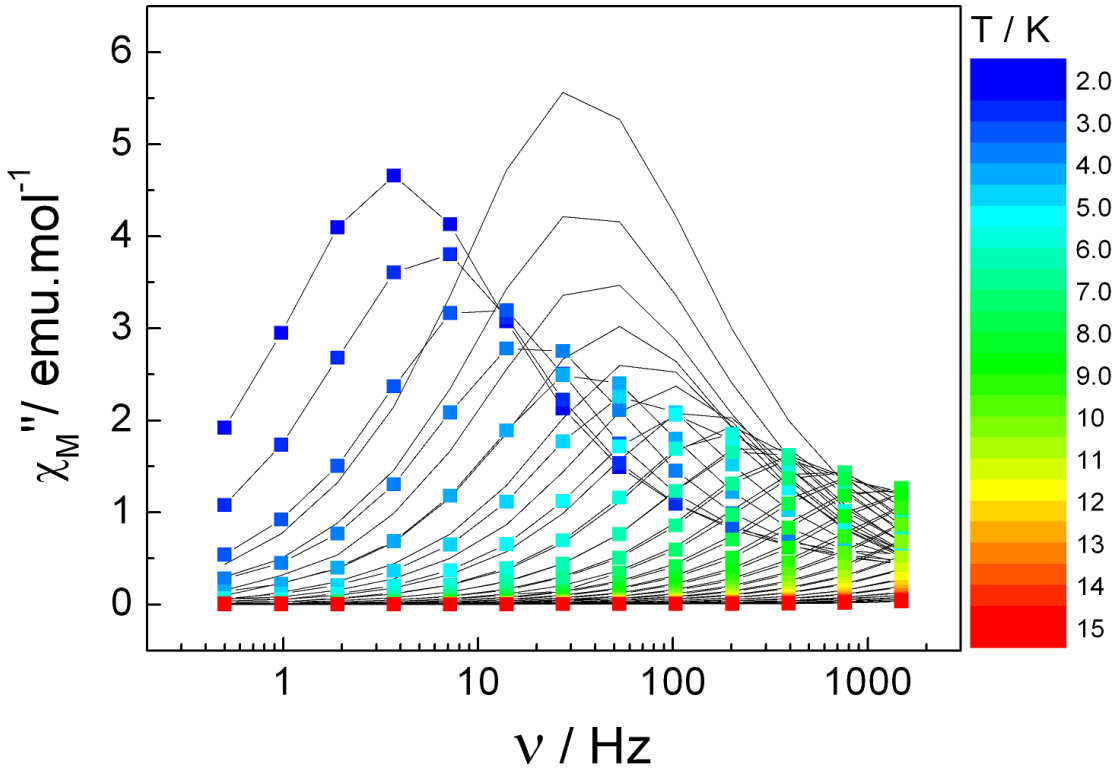

Figure S17: Comparison between the frequency dependence of χ_M'' for **1** with (lines + symbols) and without dc field (black lines).

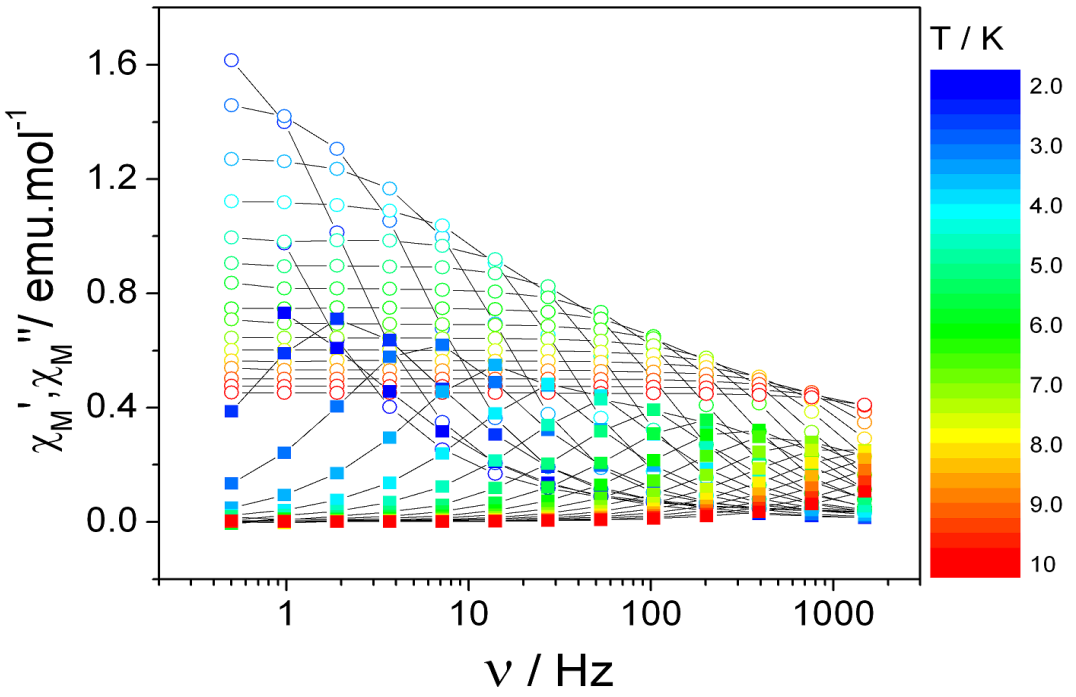

Figure S18: Frequency dependence of χ_M' and χ_M" for **2** measured with 1000 Oe external dc field. Colour mapping ranges from 2 (blue) to 15 K (red). Lines are guides to the eye.

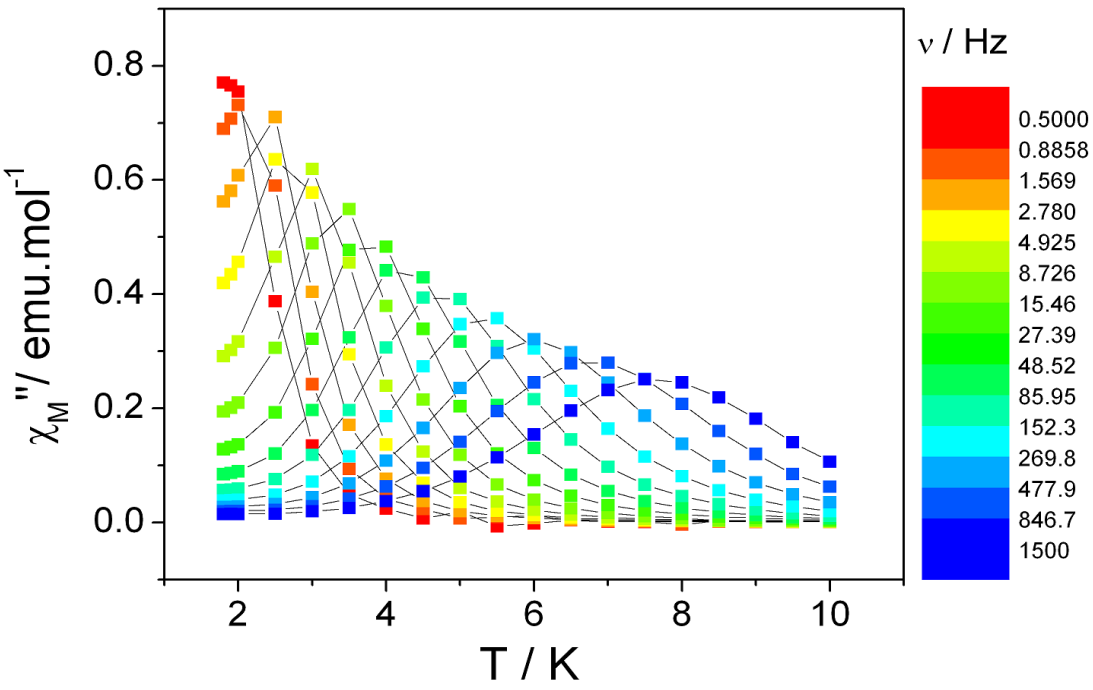

Figure S19: Temperature dependence of χ_M" for **2** measured with 1000 Oe external dc field. Colour mapping ranges from 0.5 (red) to 1500 Hz (blue). Lines are guides to the eye.

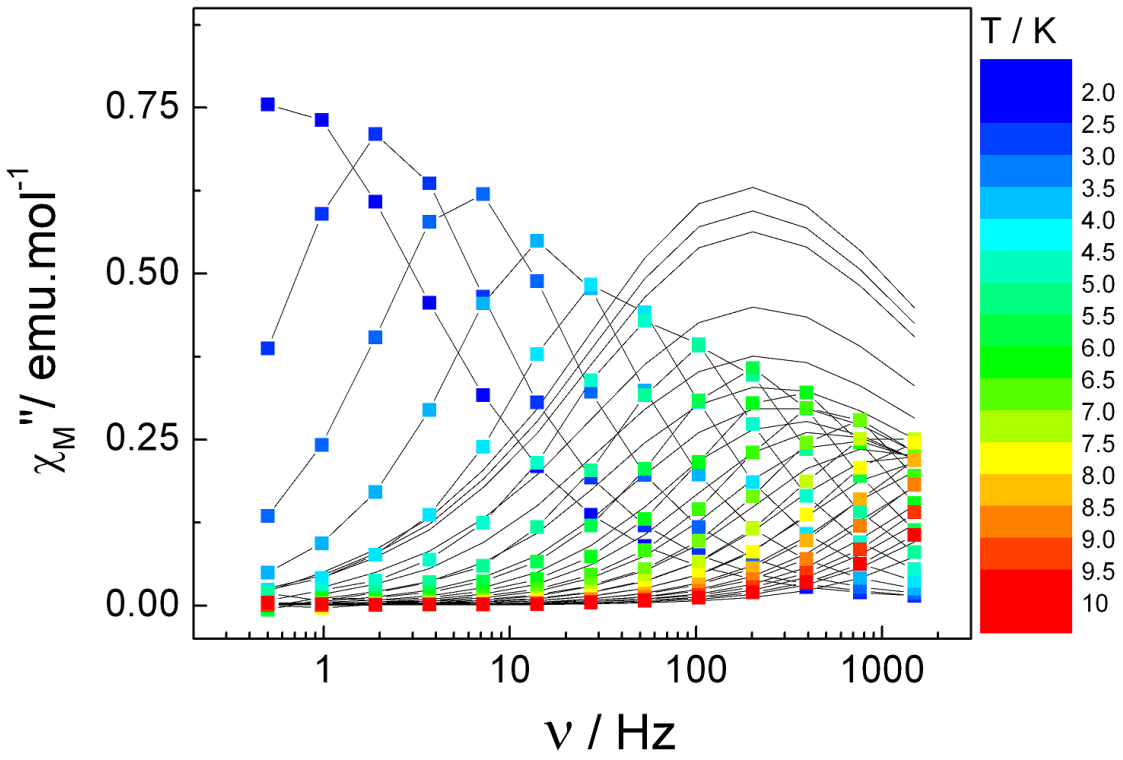

Figure S20: Comparison between the frequency dependence of χ_M" for **2** with (lines + symbols) and without dc field (black lines).

Table S8: Table of τ extracted values from the fitting of *X'' vs frequency* curves for **1** in 1000 Oe dc field.

T(K)	τ (μs)	T(K)	τ (μs)	T(K)	τ (μs)
2	42611	5	1475	8	87
2.5	26807	5.5	905	8.5	57
3	15152	6	387	9	37
3.5	8114	6.5	261	9.5	18
4	4392	7	184	10	12
4.5	2507	7.5	127		

Table S9: table of extracted values from the Argand plot of **1** with a 1000 Oe external field before normalization.

T (K)	χ_s	χ_T	α	χ^2 (x 10^{-5})
2	2.776 (±0.010)	14.883 (±0.004)	0.167 (±0.008)	1010
2.5	2.327 (±0.009)	12.063 (±0.002)	0.150 (±0.006)	353
3	2.034 (±0.011)	9.998 (±0.007)	0.119 (±0.004)	630
3.5	1.618 (±0.001)	8.502 (±0.002)	0.123 (±0.003)	573
4	1.419 (±0.003)	7.314 (±0.007)	0.094 (±0.003)	348
4.5	1.203 (±0.001)	6.434 (±0.003)	0.099 (±0.007)	221
5	0.978 (±0.002)	5.751 (±0.001)	0.099 (±0.001)	206
5.5	0.901 (±0.001)	5.194 (±0.003)	0.097 (±0.001)	122
6	0.841 (±0.005)	4.722 (±0.009)	0.086 (±0.004)	70
6.5	0.770 (±0.005)	4.333 (±0.005)	0.082 (±0.002)	130
7	0.631 (±0.002)	4.010 (±0.003)	0.101 (±0.001)	184
7.5	0.463 (±0.001)	3.728 (±0.006)	0.121 (±0.006)	190
8	0.483 (±0.002)	3.473 (±0.002)	0.097 (±0.006)	60
8.5	0.372 (±0.007)	3.087 (±0.006)	0.103 (±0.001)	40
9	0.239 (±0.001)	2.901 (±0.009)	0.102 (±0.002)	60

Table S10: Table of τ extracted values from the fitting of *X'' vs frequency* curves for **2** in 1000 Oe dc field.

T(K)	τ (μs)	T(K)	τ (μs)	T(K)	τ (μs)
2	211724	5	1389	8	104
2.5	74714	5.5	821	8.5	72
3	25852	6	511	9	48
3.5	10580	6.5	330	9.5	19
4	4911	7	220	10	8
4.5	2537	7.5	150		

Table S11: table of extracted values from the Argand plot of **2** with a 1000 Oe external field before normalization.

T (K)	χ_s	χ_T	α	χ^2 (x 10^{-5})
2	0.032 (±0.006)	2.533 (±0.005)	0.288 (±0.007)	400
2.5	0.037 (±0.001)	1.869 (±0.006)	0.186 (±0.006)	470
3	0.035(±0.001)	1.508 (±0.008)	0.121 (±0.004)	410
3.5	0.032 (±0.003)	1.282 (±0.008)	0.092 (±0.002)	160
4	0.030 (±0.004)	1.125 (±0.005)	0.081 (±0.001)	30
4.5	0.028(±0.002)	0.998 (±0.006)	0.076 (±0.007)	280
5	0.028 (±0.001)	0.898 (±0.007)	0.063 (±0.002)	90
5.5	0.023 (±0.002)	0.818 (±0.006)	0.068 (±0.003)	0.6
6	0.024 (±0.005)	0.750 (±0.003)	0.068 (±0.006)	70
6.5	0.018 (±0.008)	0.694 (±0.001)	0.075 (±0.009)	10
7	0.017 (±0.002)	0.645 (±0.001)	0.072 (±0.002)	0.1
7.5	0.012 (±0.001)	0.602 (±0.002)	0.076 (±0.009)	0.1
8	0.023 (±0.004)	0.561 (±0.001)	0.058 (±0.001)	10

Table S12: Main extracted figures from the dynamic magnetic measurements on **1** and **2**

H_{dc} (Oe)	0	0	1000	1000
Sample	Pure(1)	Doped(2)	1	2
τ_0 $(10^{-9}s)$	2.89 ± 0.02	3.40 ± 0.05	2.21 ± 0.08	2.92 ± 0.10
Δ (K)	92 ± 1	85 ± 1	91 ± 1	84 ± 1
$\tau_{(2K)}$ (Hz)	35	215	3	0.75
$\alpha_{(2K)}$	0.21	0.37	0.18	0.30
$\chi_s/\chi_{T\ (2K)}$	0.09	0.10	0.17	0.01
$\alpha_{(6.5K)}$	0.07	0.08	0.08	0.07
$\chi_s/\chi_{T\ (6.5K)}$	0.12	0.26	0.18	0.03

[1] K. Bernot, L. Bogani, A. Caneschi, D. Gatteschi, R. Sessoli, *J. Am. Chem. Soc.* **2006**, *128*, 7947-7956.

[2] A. Altomare, M. C. Burla, M. Camalli, G. L. Cascarano, C. Giacovazzo, A. Guagliardi, A. G. G. Moliterni, G. Polidori, R. Spagna, *J. Appl. Crystallogr.* **1999**, *32*, 115-119.

[3] G. M. Sheldrick, T. R. Schneider, *Methods Enzymol.* **1997**, *277*, 319-343.

[4] L. Farrugia, *J. Appl. Crystallogr.* **1999**, *32*, 837-838.

[5] T. Roisnel, J. Rodriguez-Carvajal, in *Epdic 7: European Powder Diffraction, Pts 1 and 2, Vol. 378-3* (Eds.: R. Delhez, E. J. Mittemeijer), Trans Tech Publications Ltd, Zurich-Uetikon, **2001**, pp. 118-123; bW. Kraus, G. Nolze, *J. Appl. Crystallogr.* **1996**, *29*, 301-303.